Insect Biochemistry and Molecular Biology 142 (2022) 103724

Contents lists available at ScienceDirect

Insect Biochemistry and Molecular Biology

journal homepage: www.elsevier.com/locate/ibmb

Doublesex regulates male-specific differentiation during distinct developmental time windows in a parasitoid wasp

Yidong Wang [a], Anna H. Rensink [b], Ute Fricke [a,2], Megan C. Riddle [c,1], Carol Trent [c], Louis van de Zande [b], Eveline C. Verhulst [a,d,*]

[a] Wageningen University, Laboratory of Entomology, Wageningen, the Netherlands
[b] Evolutionary Genetics, Development and Behaviour, Groningen Institute for Evolutionary Life Sciences, University of Groningen, Groningen, the Netherlands
[c] Biology Department, Western Washington University, Washington, USA
[d] Wageningen University, Laboratory of Genetics, Wageningen, the Netherlands

ARTICLE INFO

Keywords:
Nasonia
Doublesex
Sexually dimorphic traits
Sexual differentiation
Parasitoid wasps
Sex determination

ABSTRACT

Sexually dimorphic traits in insects are subject to sexual selection, but our knowledge of the underlying molecular mechanisms is still scarce. Here we investigate how the highly conserved gene, *Doublesex* (*Dsx*), is involved in shaping sexual dimorphism in the model parasitoid wasp *Nasonia vitripennis* (Hymenoptera: Pteromalidae). First, we present the revised *Dsx* gene structure including an alternative transcription start, and two additional male *NvDsx* transcript isoforms. We show sex-specific *NvDsx* expression and splicing throughout development, and demonstrate that transient *NvDsx* silencing in different male developmental stages shifts two sexually dimorphic traits from male to female morphology, with the effect being dependent on the timing of silencing. In addition, we determined the effect of *NvDsx* on the development of reproductive organs. Transient silencing of *NvDsx* in early male larvae affects the growth and differentiation of the internal and external reproductive tissues. We did not observe phenotypic changes in females after *NvDsx* silencing. Our results indicate that male *NvDsx* is required to suppress female-specific traits and/or to promote male-specific traits during distinct developmental windows. This provides new insights into the regulatory activity of *Dsx* during male wasp development in the Hymenoptera.

1. Introduction

Insects are well known for their distinct differences in male and female morphology. Reproductive organs and sexually dimorphic traits such as wing shapes and colour patterns are among the fastest evolving traits in insects and are often used to distinguish species. Development of these sexually dimorphic traits usually depends on specific genes that are expressed in a tissue- and sex-specific manner (Barmina and Kopp, 2007). Many of these genes are under control of the Doublesex (Dsx) transcription factor that initiates sexual differentiation in insects (Baker and Wolfner, 1988; Burtis et al., 1991; Clough et al., 2014; Shukla and Palli, 2012). In general, *Dsx* pre-mRNA is alternatively spliced to yield male-specific *Dsx* (*DsxM*) or female-specific *Dsx* (*DsxF*) transcripts, resulting in different sex-specific protein isoforms (Burtis and Baker, 1989; Shukla and Nagaraju, 2010a; Verhulst and van de Zande, 2015). In most insects, the splicing factor Transformer (Tra) is only functionally present in females and is responsible for female-specific splicing of *Dsx* transcripts (Hoshijima et al., 1991). In males, there is no functional Tra, and *Dsx* transcripts are spliced by default into the male isoforms (Bopp et al., 2014; Geuverink and Beukeboom, 2014; Verhulst et al., 2010b). Two functional domains are present in all insect Dsx homologs: 1) the DM domain which consists of both a DNA binding domain (DBD), and an oligomerization domain (OD1) containing a zinc module and binding sites to facilitate binding downstream targets, 2) a dimerization domain (OD2) with a common N-terminal part and a sex-specific C-terminal part (An et al., 1996; Ohbayashi et al., 2001). These C-terminal sex-specific differences are assumed to be involved in the regulation of the development of sex-specific traits (Price et al., 2015; Verhulst and van de

* Corresponding author. Wageningen University, Laboratory of Entomology, Wageningen, the Netherlands.
E-mail address: eveline.verhulst@wur.nl (E.C. Verhulst).
[1] Current addresses: Department of Psychiatry and Behavioral Sciences, University of Washington, Seattle, WA, United States of America; Eating Recovery Center 1231 116th Ave NE Suite 800, Bellevue, WA 98004.
[2] Current address: Department of Animal Ecology and Tropical Biology, Biocenter, University of Würzburg, Würzburg, Germany.

https://doi.org/10.1016/j.ibmb.2022.103724
Received 13 September 2021; Received in revised form 19 January 2022; Accepted 19 January 2022
Available online 29 January 2022

Zande, 2015). For instance, in *Drosophila,* DsxM represses and DsxF activates the expression of *bric-à-brac (bab)* which results in male-specific abdominal pigmentation (Williams et al., 2008). A similar action of Dsx is observed in the formation of sex combs, an important feature for male mating success of some *Drosophila* species (Kopp, 2011). In *Bactrocera dorsalis, Dsx* knockdown in females triggers ovipositor deformation and the interruption of yolk protein gene expression, leading to a delay in ovary development (Chen et al., 2008). These results confirm the essential role of Dsx in initiating and maintaining sex-specific development in Diptera. Also, in Lepidoptera and Coleoptera, sex-specific Dsx isoforms regulate many sex-specific traits including the development of reproductive organs and wing patterns in butterflies and moths, and mandible and head horns in beetles (Gotoh et al., 2014; Ito et al., 2013; Kijimoto et al., 2012; Kunte et al., 2014; Suzuki et al., 2005; Xu et al., 2017). Noteworthy, most of the *Dsx* knockdown experiments were conducted in a very specific developmental stage focusing on sexual differentiation; only few focused on sexually dimorphic traits. However, the expression of *Dsx* starts in early embryogenesis and continues through maturity, implying an ongoing action in regulating both sexual differentiation and the development of sexually dimorphic traits (Chen et al., 2019; Morrow et al., 2014; Robinett et al., 2010).

Thus far, the specific role of *Dsx* in regulating sexually dimorphic traits has not been studied in much detail in the Hymenoptera. *Dsx* sex-specific splice variants and expression differences have been identified in honeybees, (*Apis mellifera*), bumble bees (*Bombus ignites),* ants (*Cardiocondyla obscurior*), Japanese ants (*Vollenhovia emeryi*) and fire ants (*Solenopsis invicta*) (Cho et al., 2007; Klein et al., 2016; Miyakawa et al., 2018; Nipitwattanaphon et al., 2014; Ugajin et al., 2016), but the function of *Dsx* in regulating reproductive organ development in males has only been shown in hymenopteran sawflies, *Athalia rosae* (Mine et al., 2017, 2021). As the Hymenoptera are notable for their distinctive sexually dimorphic characters, understanding how *Dsx* directs these sex-specific and sexually dimorphic trait development in this order would add to our knowledge of the evolution of these fast evolving traits. Therefore, we used the parasitoid wasp, *Nasonia vitripennis* to 1) identify male-specific traits that are regulated by *Dsx,* and 2) study the timing by which *Dsx* regulates these traits during development.

N. vitripennis belongs to the genus *Nasonia* (*Hymenoptera: Pteromalidae*), and has become the model system for parasitoids as it is highly suitable for evolutionary and developmental genetic studies (Lynch, 2015; Werren et al., 2010). In line with all hymenopteran species, *N. vitripennis* has a haplodiploid mode of reproduction, in which females are diploid and emerge from fertilized eggs, while males are haploid and emerge from unfertilized eggs. Multiple sexually dimorphic traits within the genus *Nasonia* make it a perfect system to study sex differentiation (Darling and Werren, 1990; Raychoudhury et al., 2010). For instance, the femur and tibia of the hind legs, and the antennae of female *Nasonia* are pigmented with a dark-brown color, whereas in males these are pale yellow (Darling and Werren, 1990). Only in *N. vitripennis,* males have dramatically shorter forewings and are flightless (Darling and Werren, 1990), while the females can fly and have large forewings in all species. Previous research identified one female *Dsx* (*NvDsxF*) and one male *Dsx* (*NvDsxM*) isoform in *Nasonia*, but the identified *NvDsxM* isoform encodes only four amino acids in its sex-specific OD2 domain and its function in regulating male development is unclear (Oliveira et al., 2009), although *NvDsxM* has been implicated in the regulation of wing size dimorphism (Loehlin et al., 2010b).

To assess the role of *NvDsxM* in regulating male sexual development in more detail, we first revisited the *NvDsx* genetic structure. We confirmed existing splice-variants and identified an alternative starting exon and two additional male *NvDsx* splice-variants. We then used RNA interference (RNAi) to temporally silence *Dsx* in different male developmental stages to study its function in sexual differentiation and dimorphism. Ultimately, our results provide an important starting point to study the molecular basis of sexual differentiation and rapidly evolving sexual dimorphism in insects in general and particularly in the Hymenoptera.

2. Material and methods

2.1. Insects rearing

The *Nasonia vitripennis* lab strain AsymCx was reared on *Calliphora* sp. hosts at 16 h/8 h light/dark and 25 °C. AsymCx strain has been maintained in the laboratory for over 10 years and is cured from *Wolbachia* infection.

2.2. 5' and 3' RACE-PCR to identify additional NvDsx splice variants

For identification of the 3' ends of *NvDsx* mRNA, total RNA of three adult male- and female AsymCx wasps were extracted individually using TriZol (Invitrogen, Carlsbad, CA, USA) and cleared from genomic DNA by using the DNA-*free* DNA removal kit according to manufacturer's instructions (Invitrogen, Carlsbad, CA, USA). Total RNA was annealed with the 3' adapter from the FirstChoice RLM-RACE kit (Ambion, Austin, TX, USA) during the reverse-transcription using RevertAidTM H Minus First Strand cDNA Synthesis Kit (Fermentas, Hanover, MD, USA) and stored at −80 °C. The cDNA was subjected to series of (semi-) nested PCRs using primers complementary to the adapter and gene-specific primers targeting NvDsxU, and NvDsx_X7, NvDsx_X8 and NvDsx_X9 at 94 °C for 3 min, 35 cycles of 94 °C for 30 s, 55–62 °C for 30 s and 72 °C for 2 min, with a final extension of 10 min at 72 °C. Primers were designed based on the initial *NvDsx* gene structure (Oliveira et al., 2009) and sequences are listed in the Table S1.

For identification of the 5' end of *NvDsx*, total RNA of 3 female AsymCx wasps were extracted using TriZol (Invitrogen, Carlsbad, CA, USA). After decapping, a 45-base RNA adapter was ligated to the RNA population using the FirstChoice RLM-RACE kit (Ambion, Austin, TX, USA) and reverse transcribed using the RevertAidTM H Minus First Strand cDNA Synthesis Kit (Fermentas, Hanover, MD, USA). The cDNA was subjected to series of (semi-) nested PCRs using primers complementary to the adapter and gene-specific primers targeting *NvDsxU* at 94 °C for 3 min, 35 cycles of 94 °C for 30 s, 55–60 °C for 30 s and 72 °C for 2 min, with a final extension of 10 min at 72 °C. Primers were designed based on the initial *NvDsx* gene structure (Oliveira et al., 2009) and sequences are listed in the Table S1.

5' and 3' RACE-PCR fragments were run and visualized on ethidium bromide-containing 1.5% agarose gel with 1 × TAE buffer. All RACE-PCR products were purified using GeneJET Gel Purification Kit (Fermentas, Hanover, MD, USA) and ligated into pGEM-T vector (Promega, Madison, WI, USA) and transformed into competent JM-109 *Escherichia coli* cells (Promega, Madison, WI, USA). Colony-PCRs were conducted by using primers recommended by the kit at 94 °C for 3 min, 40 cycles of 94 °C for 30 s, 55 °C for 30 s and 72 °C for 2 min, with a final extension of 7 min at 72 °C. All isoforms were sequenced on an ABI 3730XL capillary sequencer (Applied Biosystems) and reads were visualized and aligned in MEGA4 (Tamura et al., 2007). Exon-intron structure of the genes was constructed by aligning the mRNA sequences to *N. vitripennis* genome and visualizing in Geneious Prime 2019.1.3 (http://www.geneious.com) and CLC Workbench 6.

2.3. Reverse Transcriptase-PCR (RT-PCR) to confirm usage of alternative 1' exon

Total RNA was extracted from four female samples and three male samples containing three adults each using NucleoSpin XS (Macherey-Nagel, Germany) with final elution done in 15 μl nuclease-free water. Eleven μl of eluted total RNA was converted to cDNA using RevertAidTM H Minus First Strand cDNA Synthesis Kit (Fermentas, Hanover, MD, USA) with random hexamers according to manufacturer's protocol and stored at −80 °C. One female sample was not converted to cDNA but

used as gDNA contamination control in RT-PCR. The primer sets for the RT-PCR reactions are: NvEF-1a and Nv_DsxU_F6 or Nv_DsxU_F7 with Nv_Dsx_qPCR_R (Table S1). GoTaq® G2 Flexi DNA Polymerase (Promega) was used to prepare the mastermix following manufacturer's instruction and amplified with a standard PCR profile: 3 min at 95 °C, 35 amplification cycles of 30 s at 95 °C, 30 s at 55 °C, 30 s at 72 °C and a final extension of 7 min at 72 °C in a thermal cycler (T100TM Thermal Cycler, Bio-Rad). Five μl of PCR product was visualized on a non-denaturing 1% agarose gel with a 100bp ladder. PCR fragments were Sanger sequenced at Eurofins Scientific to confirm the correct amplification.

2.4. RNAi of NvtraF and NvDsx gene

For the *Nvtra* RNAi knockdowns, MEGAscript RNAi Kit (Thermo Fisher) was used to generate dsRNA to target exon 5–8 of *Nvtra* mRNA in 4th larval instar females which resulted in a male splice form of *NvDsx* as shown in Verhulst et al. (2010a). To conduct functional analysis of *NvDsx*, same RNAi Kit was used to generate dsRNA based on either the common region of *NvDsx* (exon 2–5) that presents in both male and female splice-variants or the specific region of *NvDsx* (exon 7–9) that only presents in two longer male splice-variants. *Gfp* dsRNA was generated from the vector pOPINEneo-3C-GFP which was a gift from Ray Owens (Addgene plasmid # 53,534; http://n2t.net/addgene: 53,534; RRID: Addgene_53,534). This *gfp* dsRNA was used as control in all experiments as it has no target in *Nasonia*. Primers designed using Geneious 10.0.9 to construct the dsRNA T7 template are listed in the Table S1. For male-specific *NvDsx* RNAi, offspring of AsymCx strain was collected at 2nd and 4th larval instars and white pupa stage which are described in Table S2. All dsRNAs were diluted with RNase-free elution buffer (MEGAscript RNAi Kit (Thermo Fisher)) to 4000 ng/μl (NanoDrop™ 2000 Spectrophotometer, Thermo Fisher) before proceeding to microinjection.

Microinjection of wasps was carried out with IM300 Microinjecctor (Narishige) and FemtoJet® 4i (eppendorf) and followed the protocols described by Werren et al. (2009) and Lynch and Desplan (2006) with minor changes. Red colour food dye was pre-mixed with the dsRNAs in a ratio of 1:9. Experiments were performed using AsymCx strain at different developmental stages for different purposes (Table S3).

Second and 4th instar larvae were collected from parasitoid hosts and placed on a 1X PBS agar plate before injection. Early pupal stage samples were fixed on the glass slides with double-sided tape. After injection, 2nd instar larvae were transferred back to host (6–8 per host) and sealed with the host shell. Afterwards, sealed hosts were kept in 8 tube-PCR strips with open lid. Subsequently, all injected samples either in 8 tube-PCR strip or on slides were placed on 1 × PBS plates to prevent dehydration and incubated at standard rearing conditions until adult emergence.

2.5. NvDsx splicing and expression throughout development

Male and female wasps were separated at black pupal stage by the sex-specific traits such as forewing size and presence/absence of the ovipositor. To generate female offspring, one selected male and one selected female pupa were collected in a single glass vial clogged with cotton plug until eclosion and kept for one more day to make sure they had mated. After fertilization, two hosts per day for the first two days were provided to mated females to initiate oviposition. Afterwards,1 h host presentation was repeated twice in a row per day. Since mated *N. vitripennis* tend to lay extremely female-biased eggs, offspring from mated females was considered female (Hamilton, 1967). Under a haplodiploid mode of reproduction, virgin females produce all-male broods. In this way, male offspring was collected by using virgin females with the same setup. To facilitate early stage (eggs) sample collection, egg-laying chambers (1.5 ml Eppendorf tubes with cut-off tip presenting the head of host pupa plugged in 1000 μL filter pipet tips) were made to allow the females only access to the head portion of the fly hosts.

To confirm that male-specific splice variants are not under the regulation of NvTraF but splice in default mode independently, female samples were collected from 3 h, 1 d, 2 d, 3 d, 4 d, 5 d and 6 d after *NvtraF* knockdown. To study the expression pattern of *NvDsx* sex-specific splice variants throughout whole developmental stages, samples were collected at specific time points listed in Table S2. More than 50 embryo eggs were collected at 36 h and 5 to 10 larvae, pupae or adults were collected at 2.5 d and onwards. Collected samples were subsequently frozen in liquid nitrogen and stored in −80 °C. Sex-specific primers of *NvDsx* were designed using Geneious 10.0.9. and are listed in the Table S1. Both *NvRP49* and *NvEF-1a* were assessed for their expression stability in this semi-quantitative RT-PCR setup, and *NvEF-1a* was finally chosen as the reference gene.

Frozen samples were homogenized by pestles which were designed for 1.5 ml microcentrifuge tubes (Biosphere SafeSeal Tube 1.5 ml). Total RNA was extracted using ZR Tissue & Insect RNA MicroPrep™(Zymo) following manufacturer's instructions. On column DNase treatment step was added to all samples. Subsequently, total RNA of each samples was eluted in 16 μl of DNase/RNase free water. After verifying the purity and concentration by NanoDrop™ 2000Spectrophotometer (ThermoFisher), one μg of each template was synthesized into cDNA with a standard reaction mix (SensiFAST™ cDNA Synthesis Kit, Bioline) in a thermal cycler (Bio-Rad T100TM Thermal Cycler, Bio-Rad) with 5 min priming at 25 °C, 30 min reverse transcription at 46 °C and 5 min reverse transcriptase inactivation at 85 °C.

For all RT-PCR reactions, GoTaq® G2 Flexi DNA Polymerase (Promega) was used to prepare the mastermix following manufacture's instruction and amplified with a standard PCR profile: 3 min at 95 °C, 34 (male-specific splicing verification)/29 (expression pattern of *NvDsx*) amplification cycles of 30 s at 95 °C, 30 s at 55 °C, 50 s at 72 °C and a final extension of 5 min at 72 °C in a thermal cycler (T100TM Thermal Cycler, Bio-Rad). In order to standardize the expression pattern of *NvDsx*, the number of PCR cycles needed was determined by comparison of the brightness of the bands in gels from different PCR reactions with cycles ranging from 25 to 34 to achieve non-oversaturated brightness. In the end 29 cycles were used for both reference genes and target genes.

2.6. Silencing efficiency of NvDsx

Quantitative (q)RT-PCR was conducted to verify the silencing efficiency of *NvDsx* knockdown. After dsRNA injection, samples were collected at either adult stages (injected at the 4th larval instar and the white pupa stage) or the white pupa stage (injected at the 2nd larval instar). Four to five pupae or adults were pooled to produce one biological replicate and six biological replicates per treatment were prepared. All testing samples were used in qRT-PCR according to SensiFAST™ SYBR® No-ROX Kit manual (Bioline). *NvDsx* qRT-PCR primers were designed on the common region (exon 2–5) of male and female splice variants (Table S1). *NvEF-1a* was used as reference genes. qRT-PCR was carried out using the CFX96TM Real-Time System (Bio-Rad) with Bio-Rad CFX Manager 3.1 Software (Bio-Rad). The standard qRT-PCR profile consists of 95 °C for 3 min, 45 amplification cycles of 15 s at 95 °C,15 s of 55 °C, 30 s of 72 °C and a final standard dissociation curve step to check for non-specific amplification.

2.7. Assessment of Nasonia phenotypes

Legs, antennae, forewings and external reproduction organs of adult males were dissected on clean slides with a drop of 1 × PBS buffer using dissection tweezers, and subsequently mounted in a drop of ethanol on slides which was allowed to evaporate. Internal reproduction organs were dissected in dissection trays that were filled with 1 × PBS buffer using dissection tweezers, and were subsequently mounted in a drop of 1 × PBS on a slide and covered with a coverslip. Photos of leg, antenna, forewing and external reproduction organs were taken by Dino-Lite

Edge 5 MP digital microscope and measured by using DinoCapture 2.0 software. Photos of internal reproduction organs were captured by the sCMEX-20 camera (Euromex Scientific) coupled with a Leitz Dialux 20 EB light microscope and generated in ImageFocusAlpha software. Zerene Stacker was used for photo stacking. Forewing size was measured by wing length and width based on the standard methods described by Loehlin et al. (2010a). Tibia length of the hind leg was used to standardize the body size differences among individuals (Godfray, 1994). Reproduction apparatuses were identified based on the description in Liu et al. (2017) and E. Snodgrass (1957).

2.8. Data analysis

qRT-PCR data was first imported to LinRegPCR software (LinRegPCR, 2017.1.0.0, HFRC, Amsterdam, The Netherlands) (Ramakers et al., 2003). After baseline correction, the initial number of templates (N0) were calculated based on the average PCR efficiency of each amplicon. Relative expression levels of *NvDsx* in each sample was obtained by dividing the N0 value of *NvDsx* by N0 value of *NvEF-1a*. Statistical analysis of qRT-PCR and measurement data was performed in R using One-way ANOVA and Tukey's Honest Significant Difference (HSD) for post-hoc test.

3. Results

3.1. Identification of two additional male-specific Dsx splice variants

Previously, only one female (*NvDsxF*) and one male (*NvDsxM*) *Dsx* splice forms were identified in *N. vitripennis* (Oliveira et al., 2009). The *NvDsxF* splice variant shares the same first four exons with the *NvDsxM* splice variant, but 108 bases are spliced out from exon 5 which leads to female-specific exons 5F and 6F. In *NvDsxM,* exon 5M results from retention of this 108bp intron, and the entire transcript encodes a Dsx protein with a very short OD2 domain of only four amino acids (aa). This intron retention does not resemble any Dsx splice variant in other insect orders (Oliveira et al., 2009) (Fig. 1, *NvDsxF* and *NvDsxM1*). To investigate the possibility of additional splice variants of *Dsx* pre-mRNA in *N. vitripennis,* we performed extensive 5' and 3' Rapid Amplification of cDNA Ends (RACE). The results reveal a novel alternative starting exon that we designated exon 1' (Fig. 1). Using RT-PCR to target exon 1' to exon 5, we verified its presence in transcripts of both sexes but with a higher frequency in female transcripts (Fig. S1). Alternative splicing at the 5' end has not been shown for *Dsx* before, but it does not change the start codon of Dsx protein translation. From here on we refer to the alternative variants collectively. 3' RACE yielded two additional male splice variants (Fig. 1). We designated the previously published male-specific variant *NvDsxM1* (M1: NM_001162517; M1': MT043363); the longer male splice forms we present here are designated *NvDsxM2* (M2: MT043359; M2': MT043360) and *NvDsxM3* ((M3: MT043361; M3': MT043362). All male isoforms share the same exons 1 (or 1') to 5 with the female isoform *NvDsxF* (F: NM_001162518; F': MT043364). The *NvDsxM2* open reading frame ends with a stop codon in exon 8 and translates into a protein of 328 aa which is 105 aa longer than the open reading frame of *NvDsxM1*. In *NvDsxM3,* compared to *NvDsxM2,* exon 8 is spliced out and the stop codon is encoded in exon 9, yielding a protein of 330 aa. NvDsxM2 and NvDsxM3 protein isoforms are almost completely identical and only differ at the C-terminus downstream of the male-specific OD2 domain.

To determine whether the newly identified splice variants are exclusively expressed in males, we observed the overall expression of different *NvDsx* splice forms in both males and females. Across development, *NvDsxF* is only expressed in females while *NvDsxM1, NvDsxM2* and *NvDsxM3* are highly expressed in males (Fig. S2), but expressed at a very low level in females. In males an increase of *NvDsxM1, -2 and -3* expression from 36h toward the 4th instar larvae was observed (Fig. S2). Afterwards, the expression remains relatively constant until adult stage (Fig. S2). Overall, *NvDsxM2* is more abundant than *NvDsxM3* (Fig. S2). Females express *NvDsxM1*, *NvDsxM2* and *NvDsxM3* at a very low level probably due to leaky default splicing of male-specific transcripts (Fig. 2B and Fig. S2).

We have shown previously that parental *Nvtra* RNAi in the female pupal stage leads to a significant ~65% reduction of *Nvtra* expression and a shift in splicing from *NvtraF* to *NvtraM* (Verhulst et al., 2010a). This subsequently induces a shift from *NvDsxF* to *NvDsxM* (now *NvDsxM1*) splicing in both the treated adult females and the offspring, without consequences for adult female fertility (Verhulst et al., 2010a). The reduced levels of NvtraF are no longer sufficient to regulate the splicing of all *NvDsx* transcripts into the female-specific form, leading to default expression of *NvDsxM1* splice variants. To verify the default and NvTraF independent splicing of *NvDsxM2* and *NvDsxM3*, we silenced *Nvtra* in 4th instar female larvae. We assessed the different *NvDsx* and *Nvtra* splice variants from 3 h post injection (hpi) to 5 days post injection (dpi) using RT-PCR. We affirmed that *Nvtra* RNAi leads to *NvtraM* splicing in females (Fig. 2A) and observed a minor increase of *NvDsxM1*

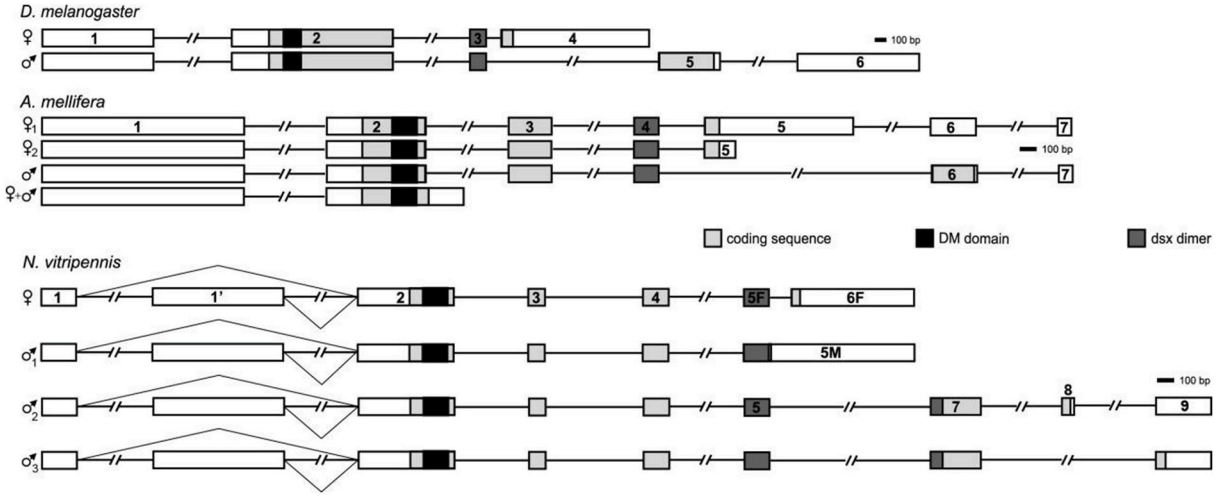

Fig. 1. Comparison of insect *Doublesex* (*Dsx*) gene models. The eight *N. vitripennis* male and female *Dsx* splice variants are compared to *Dsx* splice variants of *D. melanogaster* and *A. mellifera*. Figure was modified from Oliveira et al. (2009) to include the alternative 1st exon (1') and the additional *NvDsx* male splice variants. Male and female specific splice forms are indicated by ♂ and ♀. Exon numbers are noted on each exon. Light grey, black and dark grey blocks indicate coding region, DM domain and OD2 Dsx dimer region respectively. Scales are provided behind each species splice structures.

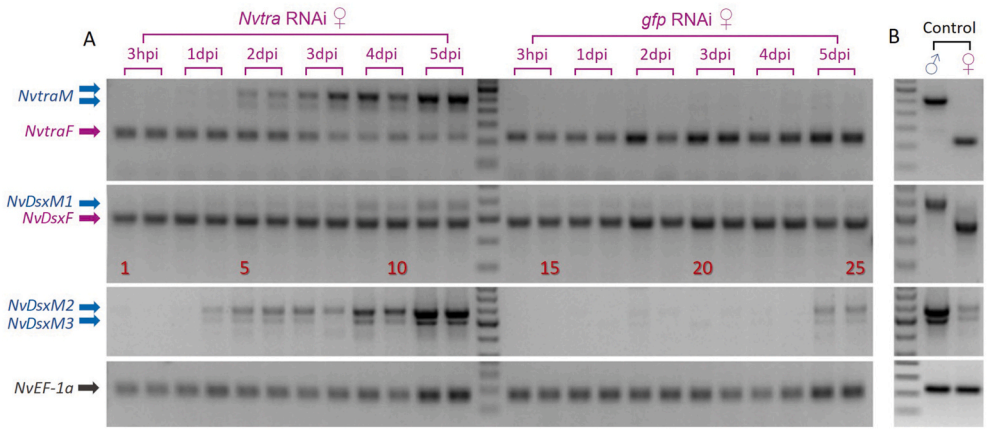

Fig. 2. Confirmation of sex-specific *Dsx* splicing after *Nvtra* knockdown in *N.vitripennis*. (A) Sex-specific splice variants of *Nvtra* and *NvDsx* in *N. vitripennis* females that are injected in the 4th instar larval stage with *Nvtra* dsRNA or *gfp* dsRNA. (B) Male and female non-treated (NT) control samples for each primer sets. Arrows indicate male (in blue) and female (in purple) splice forms of the different genes. Lanes 1–12: Female *Nvtra* knockdown samples from 3 h post injection (hpi) to 5-day post injection (dpi). Lane 13: 100bp ladder (Thermo). Lanes 14–25: Female *gfp* knockdown samples from 3dpi to 5dpi. For each stage two samples are used. *NvEF-1a* is used as expression and loading control.

expression from 4 dpi onwards, while *NvDsxM2* and *NvDsxM3* expression levels increase substantially from 1dpi onward compared to mock *gfp* RNAi (Fig. 2A). We did not observe a clear reduction in female *NvDsxF* splicing (Fig. 2A).

3.2. Effects of NvDsx RNAi in males depend on the timing of injection

To assess the sex-specific function of Dsx, we started by silencing *NvDsx* using RNAi in different developmental stages (Fig. S3*A,B,C*) and determined *NvDsx* silencing by qRT-PCR in later stages. We were unable to silence the male-specific splice variants of *NvDsx* specifically (*NvDsxM*-i, Fig. S3*B*), so we targeted the common region of *NvDsx* by injecting *NvDsxU* dsRNA (from here on indicated as *NvDsx*-i). We observed that the developmental stage at which *NvDsx*-i was done, greatly influenced the expression levels of *NvDsx* we measured using qRT-PCR five to seven days later. First, we injected 2nd instar male larvae with dsRNA against *NvDsx* or *gfp* (mock) and sampled these males five days later when they were in the white pupal stage to assess *NvDsx* expression levels. We found no significant decrease of *NvDsx* expression in comparison to non-treated (NT) and *gfp* mock (*gfp*-i) (Fig. S3*A*) in these males. It could be that the strong increase in male *NvDsx* expression from 4th instar larvae onwards (Fig. S2) is the main cause as the limited amount of siRNA present in the 2nd larval instar is not capable of silencing the increase of transcript numbers in later developmental stages. Next, we performed *NvDsx*-i in 4th instar male larvae, which is one day prior to pupation, and sampled these males seven days later as newly emerged adults to assess *NvDsx* expression. In this case we observed a significant reduction of *NvDsx* when compared with both NT (Tukey's HSD, $P < 0.001$) and *gfp*-i males (Tukey's HSD, $P < 0.001$) (Fig. S3*B*). It confirmed a successful *NvDsx* knockdown starting in 4th instar male larvae with an effect lasting into adulthood. Finally, we treated white pupal stage males with *NvDsx*-i and sampled at the adult stage (six days after injections). We observed a significant reduction of *NvDsx* expression when comparing *NvDsx*-i to NT (Tukey's HSD, $P = 0.003$) and pupal stage *gfp*-i males (Tukey's HSD, $P = 0.002$) (Fig. S3*C*) which indicates that we also obtained a highly significant knockdown of *NvDsx* from the pupal stage onwards. The transient nature of RNAi in *Nasonia* allows us to suppress *NvDsx* during specific developmental time windows to assess the effects on morphological development. Our experimental setup is therefore different from many genome editing studies in which *Dsx* is knocked out from early embryogenesis onwards (Chen et al., 2019; Xu et al., 2017).

3.3. Silencing NvDsx in males results in female-like morphological trait development

After determining the silencing of *NvDsx* after RNAi at three different developmental stages, we continued by observing the morphological changes after *NvDsx*-i in males of the different developmental stages. We observed changes in antenna pigmentation, and femur and tibia pigmentation of the hind legs (hereafter legs); we did not find any pigmentation changes in other body parts. NT and *gfp*-i males showed unpigmented antennae and legs (Fig. 3*A,B,C*), whereas NT females have pigmented antennae and legs (Fig. 3*D*). *NvDsx*-i in 2nd instar male larvae increased the amount of pigmentation in the adults slightly (Fig. 3*F*), even though we did not observe a significant reduction in *NvDsx* expression in these samples at white pupal stage (Fig. S3*A*). Silencing *NvDsx* from 4th instar male larvae onwards resulted in female-like pigmentation in the adult stage (Fig. 3*E*). When we silenced *NvDsx* from the white pupal stage onwards we did not see an increase in pigmentation (Fig. S4*G*), suggesting that upon pupal metamorphosis the developmental window of NvDsx regulation on sex-specific pigmentation is closed.

Then we observed changes in forewing size and shape in *N. vitripennis* adult males following *NvDsx*-i in different developmental stages. Silencing *NvDsx* in both 2nd and 4th instar larvae resulted in increased forewing length and width of adult males when compared to *gfp*-i (Tukey's HSD, $P < 0.001$) and NT males (Tukey's HSD, $P < 0.001$) (Fig. 4*B,C*). Length/width (L/W) ratio of *NvDsx*-i treatments showed severe reduction compared to *gfp*-i (Tukey's HSD, $P < 0.001$) and NT males (Tukey's HSD, $P < 0.001$) (Fig. 4*A*), indicating that the forewing became wider and more female-like. However, the forewings of the *NvDsx*-i males were still smaller and narrower than those of the NT females (Length: Tukey's HSD, $P < 0.001$; Width: Tukey's HSD, $P < 0.001$; L/W ratio: Tukey's HSD, $P < 0.001$) (Fig. 4*A,B,C*). Interestingly, also here we found an effect of *NvDsx*-i timing as the forewing length and width increased significantly between 2nd and 4th instar treated larvae, with earlier stage *NvDsx* knockdown leading to more severe changes (Tukey's HSD, $P < 0.001$), steering the L/W ratio towards NT females dramatically (Tukey's HSD, $P < 0.001$). No significant differences were observed between 2nd and 4th instar *gfp*-i males (Tukey's HSD, $P = 0.062$), 2nd instar *gfp*-i and NT males (Tukey's HSD, $P = 0.070$) and 4th instar *gfp*-i and NT males (Tukey's HSD, $P = 0.999$) (Fig. 4*A,B,C*). Silencing *NvDsx* in the white pupal stage had no effect on forewing size or shape in adult males (Fig. S4), suggesting that the developmental window of NvDsx regulation on sex-specific wing size is also closed upon pupal metamorphosis.

3.4. Silencing NvDsx affects growth and development of male genitalia

Next, we assessed the role of *NvDsx* in male genitalia development by silencing *NvDsx* in the 2nd and 4th instar larval stage. *NvDsx*-i in both developmental stages reduced the aedeagus length significantly when compared to *gfp*-i in both developmental stages and NT males (Tukey's HSD, $P < 0.001$) (Fig. 5*A,B*). *NvDsx*-i males from both developmental stages had the same extent of aedeagus length reduction (Tukey's HSD,

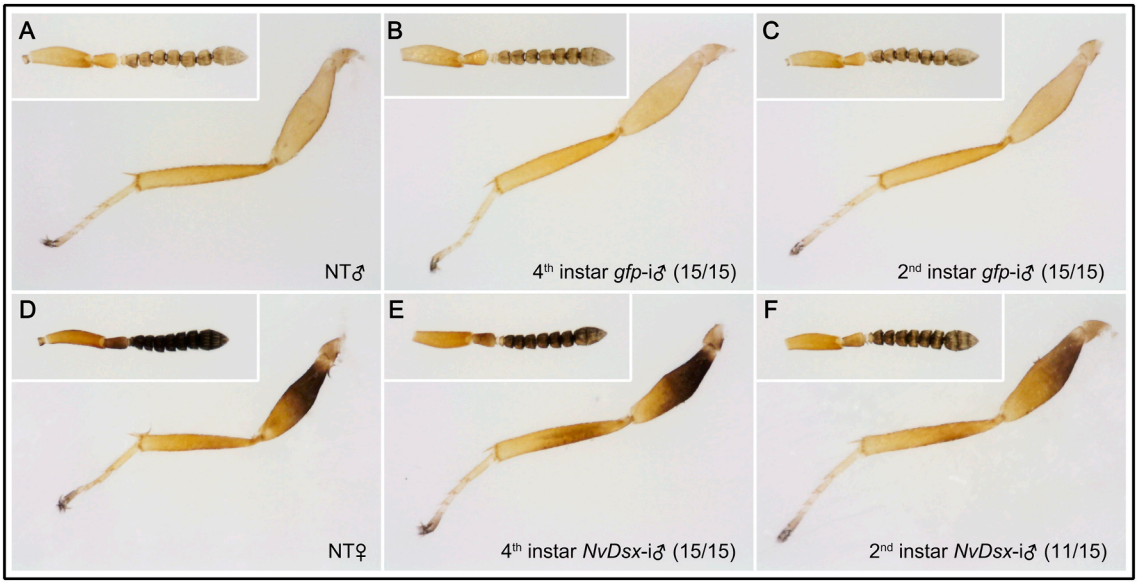

Fig. 3. Pigmentation of antennae and hind legs of adult wasps after *NvDsx* or *gfp* dsRNA treatment in different developmental stages. (A) non-treated (NT) male (B) 4th instar *gfp* RNAi (*gfp*-i) male (C) 2nd instar *gfp*-i male (D) NT female (E) 4th instar *NvDsx* RNAi (*NvDsx*-i) male and (F) 2nd instar *NvDsx*-i male. Light source and exposure time are equal for all pictures. The number of individuals that emerged with representative phenotypes against the total number of examined individuals are provided in the figure. The result is replicated three times in the laboratory.

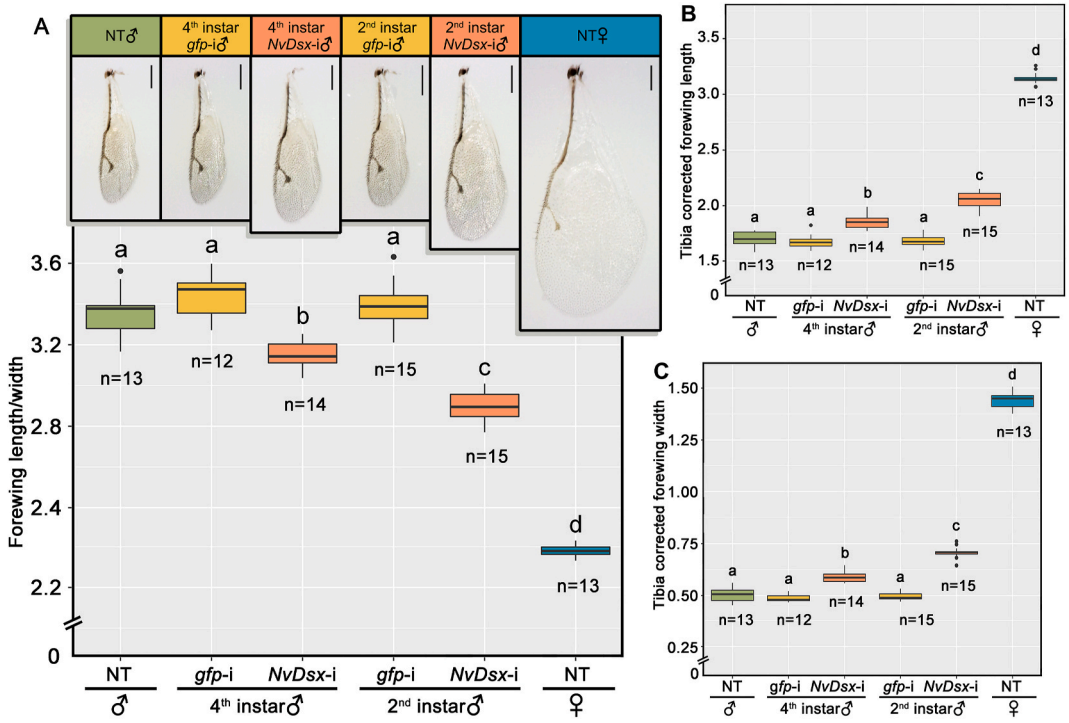

Fig. 4. Comparison of forewing size of adult after *NvDsx* or *gfp* dsRNA treatment in the 2nd or 4th larval instar males and non-treated control. Y-axis represents: (A) Depiction of forewings of different RNAi treatments and the forewing length/width ratio corrected with tibia length, (B) Wing length corrected with tibia length, (C) Wing width corrected with tibia length. X-axis shows six groups: males treated with dsRNA of *NvDsx* (*NvDsx*-i) and *gfp* (*gfp*-i) in the 2nd and 4th larval instar, non-treated (NT) males and NT females. Wing sizes were corrected with tibia length and scales indicate 200 μm. Boxplots were generated in R and display minimum, first quartile (Q1), median, third quartile (Q3), and maximum. Dots outside the boxplots represent outliers. Replicates are provided in the figures of each treatment. One-way ANOVA and post-hoc Tukey's HSD were used for data analysis. Letters in the figures denote statistical significance ($P < 0.05$) among treatments. The result is replicated three times in the laboratory.

$P = 0.998$). Aside from the shortened aedeagus, the paramere (genital organ structure without aedeagus) was also severely reduced in size in both 2nd and 4th instar *NvDsx*-i males compared to *gfp*-i and NT males (Fig. 5*C*), whereas the structure of the paramere including the outer parameres, cuspis and digitus, was still intact (Fig. 5*C*). Interestingly, unlike the aedeagus differences, the 2nd instar *NvDsx*-i males displayed more dramatic reduction in size of the outer paramere than the 4th instar *NvDsx*-i samples (Tukey's HSD, $P < 0.001$, Fig. 5*D*). We recorded the

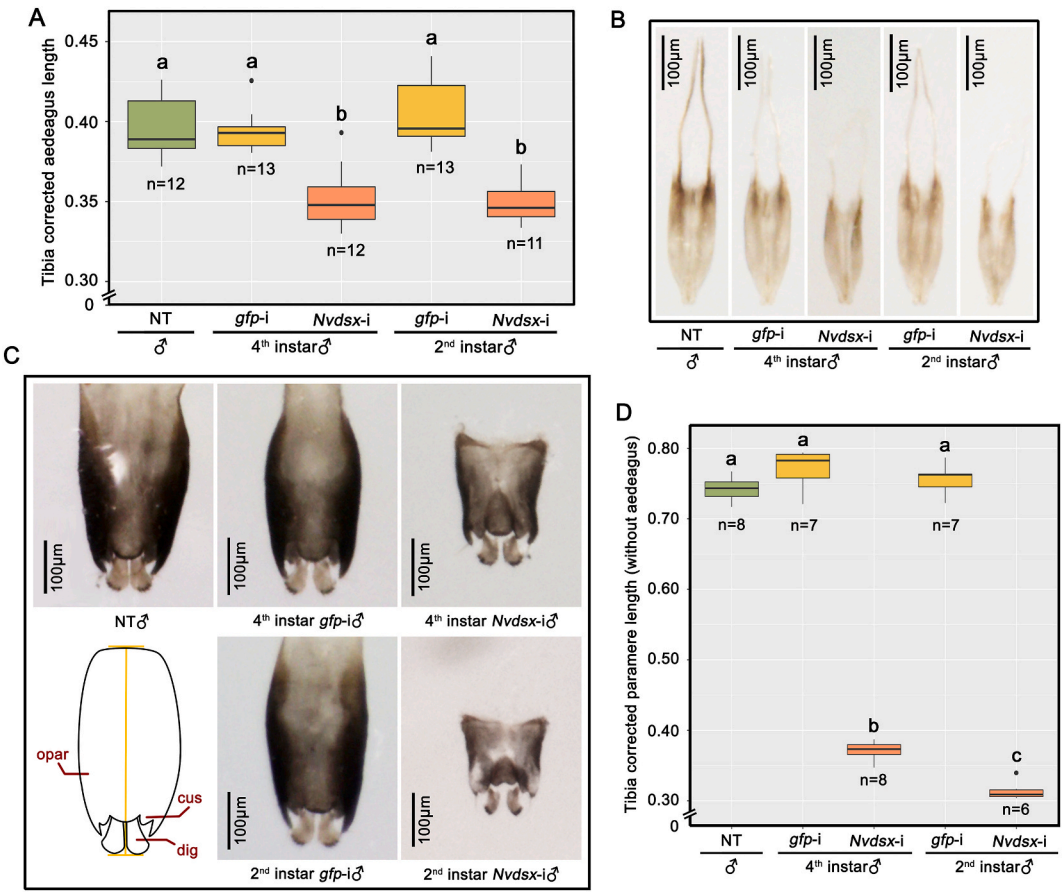

Fig. 5. Comparison of external reproductive organs in males of different treatments. (A) Comparison of genitalia length of adult males treated with *NvDsx* dsRNA (*NvDsx*-i) or *gfp* (*gfp*-i) in the 2nd or 4th larval instar males and non-treated (NT) control males. Y-axis represents genitalia length corrected by tibia length. Comparison of (B) aedeagus length and (C) paramere length (without aedeagus) of adult males after *NvDsx* or *gfp* dsRNA treatment in the 2nd or 4th larval instar and NT control. Each paramere component is described in Snodgrass (1957) and labeled with the following abbreviations: outer paramere (opar), cuspis (cus) and digitus (dig). The length of the opar is indicated by the yellow line. Scales are provided in the photos. (D) Comparison of paramere length (without aedeagus) of adult males treated with *NvDsx* dsRNA or *gfp* in the 2nd or 4th larval instar males and NT control males. Y-axis represents paramere length (without aedeagus) corrected by tibia length. All boxplots were generated in R and display minimum, first quartile (Q1), median, third quartile (Q3), and maximum. Dots outside the boxplot represent outliers. One-way ANOVA and post-hoc Tukey's HSD were used for data analysis. Letters in the figures denote statistical significance ($P < 0.05$) among treatments. The result is replicated three times in the laboratory.

mating ability of the *gfp*-i (Movie S1) and *NvDsx*-i (Movie S2) males and observed that the severe length reduction of the genitalia rendered *NvDsx*-i males unable to copulate with females, showing that in this case size matters. Taken together, these results suggest that the NvDsx regulatory window of aedeagus growth in *N. vitripennis* males continues into pupation, while the paramere growth is regulated mostly during larval development.

Finally, we assessed the effect of *NvDsx* silencing at different developmental stages on the internal reproductive tissue development in the adult stage. Compared to the reproductive tissue development from normal female (Fig. 6*A*), normal male (Fig. 6*B*) and *gfp*-i males (Fig. 6*D, F*), it was clear that the most pronounced effect was in the 2nd larval instar *NvDsx*-i males. In these males a severely deformed testis resembling more a female-like ovary structure is observed (Fig. 6*E*). Seminal vesicles are also malformed and resemble a female-like lateral oviduct (Fig. 6*E*). In comparison, 4th larval instar *NvDsx*-i males develop a mostly normal formed testis structure (Fig. 6*C*), however the seminal vesicles in 4th larval instar *NvDsx*-i males are smaller in size and do not contain any observable mature sperm (Fig. 6*I*) when compared to *gfp*-i males (Fig. 6*H*) and NT males (Fig. 6*G*). These results suggest that the NvDsx regulation of sex-specific reproductive tissue development ends around pupal metomorphosis, but NvDsx role in regulating sperm maturation continues most likely into adulthood.

3.5. Silencing NvDsx has no effect on sexually dimorphic trait development in females

To get a full picture of the role of NvDsx in regulating sexually dimorphic traits in both sexes, We also silenced *NvDsx* in 4th instar females. Although a previous study showed that RNAi in females is effective (Verhulst et al., 2010a), here we found that the efficiency of *NvDsx* RNAi in females is low (Fig. S5*I*), with *NvDsx* expression being significantly different compared to non-treated females (Tukey's HSD, $P = 0.006$), but not to *gfp*-i females (Tukey's HSD, $P = 0.052$). We did not observe phenotypic changes as a result of *NvDsx*-i, and the females had normal levels of antennae and leg pigmentation (Fig. S5G) when compared to non-treated (Fig. S5*A*) and *gfp*-i (Fig. S5*E*) females. Similar for wing size, no change was observed in wing size (Fig. S5*B, F* and *H*) nor shape (Fig. S5*K, J* and *L*) when comparing non-treated and/or *gfp*-i treated females to *NvDsx*-i treated females. We also did not observe differences in external or internal reproductive organs when comparing non-treated, *gfp*-i treated and *NvDsx*-i treated females, with all females having a normal shaped ovipositor (Fig. S6*D-F*) and fully developed ovaries (Fig. S6*A-C*).

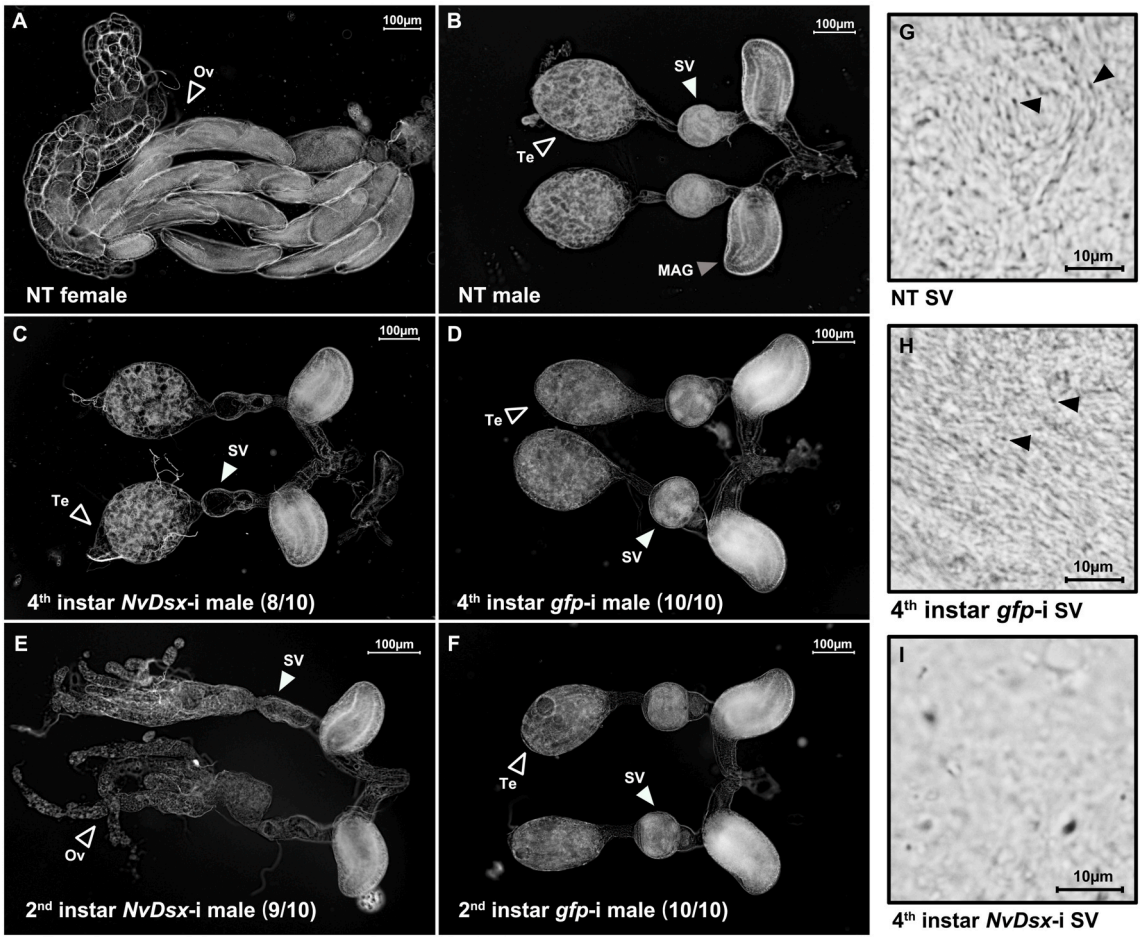

Fig. 6. Structure of the internal reproduction organs shown for (A) non-treated (NT) female, (B) NT male, (C) male treated with *NvDsx* dsRNA (*NvDsx*-i) and (D) *gfp* (*gfp*-i) in the 4th larval instar, (E) *NvDsx*-i male and (F) *gfp*-i male in the 2nd larval instar and the comparison between (G) NT male, (H) 4th instar *gfp*-i male and (I) 4th instar *NvDsx*-i male seminal vesicle. MAG, SV and Te refers to male accessory gland, seminal vesicle and testis. Active spermatozoa in the NT male seminal vesicle are indicated with black arrows (G). Scales are provided in the photos. The number of individuals that emerged with representative phenotypes against the total number of examined individuals are provided in the figure. The result is replicated three times in the laboratory.

4. Discussion

In this study we set out to assess the role of male-specific *Dsx* isoforms in regulating male sexual dimorphism and sexual differentiation in *N. vitripennis*. In addition to the already known very short male-specific isoform, we identified two additional male-specific NvDsx isoforms with full-length OD2 domains. Within insects *Dsx* splice variants often differ in terms of structure and number. *N. vitripennis* expresses three male and one female sex-specific splice form of *Dsx,* but contrastingly, *D. melanogaster* has only one male-specific and one female-specific splice form described (Burtis and Baker, 1989). The two newly identified male-specific *NvDsx* splice variants skip the female-specific exon 6 completely, yet this is a shared feature of male-specific splicing in many insect species including fruit flies (*D. melanogaster*) (Burtis and Baker, 1989) and honeybees (*A. mellifera*) (Cho et al., 2007), but also wild silkmoths (*Antheraea assama*) (Shukla and Nagaraju, 2010b) and fire ants (*S. invicta*) (Nipitwattanaphon et al., 2014). We did not find any non-sex-specific splice variants in *N. vitripennis* as opposed to *A. mellifera* (Cho et al., 2007). Then, the *NvDsxM1* isoform retains a 108bp intron that is spliced out from *NvDsxF*, and a similar splicing mechanism was also observed in *A. rosae* in which exon 5 (119bp) is retained in males but spliced out in female-specific *Dsx* splice variants (Mine et al., 2017). In both cases this intron retention creates early in-frame stop codons resulting in a very short male-specific OD2 domain. The mechanism by which this short male-specific isoform would perform its sex-specific regulatory function in *N. vitripennis* is unclear, and future research will depend on gene editing techniques, such as CRISPR/Cas9 (Chaverra-Rodriguez et al., 2020; Li et al., 2017), to mutagenize these different *NvDsx* isoforms to study their roles in sexual development.

4.1. Pigmentation

The observation that silencing *NvDsx* induced complete female-like pigmentation in males leads us to conclude that female-specific pigmentation is actively suppressed by NvDsx in male *N. vitripennis*, most likely by interfering with the melanin synthesis pathway. This observation is corroborated by the lack of pigmentation changes in *NvDsx* silenced females, although *NvDsx* RNAi silencing efficiency in females is only moderate. Pigmentation is a highly variable trait among diverse insect species. It provides physical protection through e.g. thermoregulation, UV protection and desiccation resistance (True, 2003). In *D. melanogaster,* sex-specific pigmentation of the abdominal segments is regulated by interaction of the HOX protein Abdominal-B (Abd-B) and Dsx (Kopp et al., 2000). However, in this case DsxM activates the pigmentation pathway leading to abdomen pigmentation in males only (Kopp et al., 2000; Williams et al., 2008). Although the pigmentation intensity of the legs is similar in appearance between NT females and 4th instar *NvDsx*-i males, we observed a slight reduction in antenna pigmentation of 4th instar *NvDsx*-i males (Fig. 3*E*). This can be caused by 1) a structural difference in the antennae with males having

less plate organs on the sub-segments than females, causing a different color reflection (Slifer, 1969); or 2) incomplete penetrance of *NvDsx*-i in head tissue. We suggest that the less intense pigmentation in the legs of 2nd instar *NvDsx*-i males is due to the transient nature of RNAi, in which the *NvDsx* silencing effect was already diminished but the still reduced levels of NvDsx protein could mildly repress the pigmentation pathway. No pigmentation was observed in the adults of early pupa stage *NvDsx*-i males indicating that NvDsx fully repressed the pigmentation pathway before the RNAi silencing could take effect. Although the deposition of the pigments in the cuticle often starts from late pupal to early adult stages (Massey and Wittkopp, 2016), our results suggest that *NvDsx* represses the pigmentation pathway in male larvae before pupal metamorphosis.

4.2. Forewing size

Previous research showed that backcrossing the *N. giraulti wing-size1* locus (*ws1*), a non-coding region of *Dsx,* into the *N.vitripennis* genetic background is correlated with the development of larger wings in *N. vitripennis males* (Loehlin et al., 2010b). Although higher *NvDsxM1* expression levels were detected in individuals with the *N. vitripennis ws1* variant (Loehlin et al., 2010b), the mechanism of wing size regulation by NvDsx is unclear and the *NvDsxM2* and *-3* splice variants were unknown at the time. Our research confirmed that high *NvDsx* levels in males are required for the regulation of the male forewing size by repressing wing growth. In addition, the sex-specific *widerwing* (*wdw*) locus has been backcrossed from *N. giraulti* into *N. vitripennis* thereby increasing male but not female forewing width (Loehlin et al., 2010a), with *wdw* encoding an *upd-like* growth gene (Loehlin and Werren, 2012). The increase of the wing size by introducing either *wdw* or *ws1* from *N. giraulti* to *N. vitripennis* background is due to the growth of both the cell size and the cell number (Loehlin et al., 2010a, 2010b). We observed that 2nd instar *NvDsx*-i males developed larger, more female-like wings than 4th instar *NvDsx*-i males, but an increase in wing size and width was observed for both treatment groups. This can be explained by the requirement for continuous repression of NvDsxM1-3 on imaginal wing disc growth throughout larval development in males. Silencing *NvDsx* in males abolishes the repression of wing growth, thereby promoting it. For *D. melanogaster* it has been shown that the wing imaginal disc cells experience an exponential growth from the beginning of larval development until pupal metamorphosis, (Garcia-Bellido and Merriam, 1971). In *N. vitripennis* this would then result in an incomplete female-specific wing phenotype as male-specific wing disc development started well before the applied 2nd instar *NvDsx*-i window. However, we did not observe any reduction in female forewing size when we silenced *NvDsx* in females, although we could not obtain a high RNAi silencing efficiency. Still, the antagonistic effects of NvDsxM and NvDsxF may play a role in wing size development in *Nasonia*, as has been shown for *Aedes aegypti* females, in which *Dsx* knockdown leads to smaller wing development (Mysore et al., 2015). The downstream target genes that are regulated by NvDsx in males to repress wing growth are currently unknown and require further investigation.

4.3. External genitalia

Dsx is known to be involved in the differentiation of external genitalia structures in male and female insects (Christiansen et al., 2002), however, whether *Dsx* is continuously required for genitalia development has not received much attention. Previous studies using *Dsx* RNAi experiments in other species were conducted at late larval stages and resulted in either deformed external genitalia or chimeras that contain the structures of both sexes (Mine et al., 2017; Zhuo et al., 2018). In contrast, in *N. vitripennis* males, both 2nd instar and 4th instar *NvDsx*-i treatments result in only a size reduction of the external genitalia, but have no visible effect on morphology. In the first larval instar of *D. melanogaster*, *Dsx* expression is already detected in the first few cells of the genital disc (Robinett et al., 2010), which later directs the differentiation of genital primordia (Keisman et al., 2001). The Dsx-induced regulation starts relatively early to determine the sex-specific fate of the genitalia development (Keisman and Baker, 2001). This likely explains the absence of male external reproductive tissue deformation in our study. We suggest that in *N. vitripennis* the sexual differentiation of male external genital organs is determined well before 2nd instar larval stage, but sex-specific input from NvDsx is constantly required during development for male external genitalia growth. In addition, our results show that there is a slight difference in the exact NvDsx regulatory window of male genitalia growth. The window in which *NvDsx*-i can affect paramere growth is larger than that for aedeagus growth, indicating the delicate regulation of NvDsx on the growth of sex-specific traits.

4.4. Internal genitalia

Contrary to its regulation of growth of external genitalia, NvDsx regulates the morphology of the internal genitalia during larval development. Silencing the *NvDsx* in 2nd instar *N. vitripennis* males resulted in a significant effect on internal genitalia with a female-like ovarian structure and malformed seminal vesicles. Silencing *NvDsx* in 4th instar larvae has a less pronounced effect, although we observe testis shape malformation and sperm production impairment. In both treatments, the accessory glands remain intact.

The role of Dsx in regulating the development of internal genitalia in insect has only been thoroughly studied in *Drosophila*, in which gonads develop from a combination of germ cells and somatic gonadal precursors (SGPs) (Whitworth et al., 2012). Sexual differences in gonad size can already be seen during early larval stage (Kerkis, 1931), as a consequence of the presence of male-specific SGPs (DeFalco et al., 2003). Although this sexual dimorphism is established in early development, the cells in the gonad remain highly plastic in their sexual development until late larval stage (Camara et al., 2019). Furthermore, in *Drosophila,* seminal vesicles also show a potential for later sexual differentiation as a recruitment of mesodermal cells into genital disc happens in the last larval stage, after which these recruited cells eventually contribute to major parts of the internal genitalia (Ahmad and Baker, 2002). This could explain our observation of different development time window in which NvDsx regulates external and internal genitalia differentiation. Recently, Mine et al. (2021) found that reducing the expression of *ArDSX* in male *A. rosae* leads to the complete development of female internal reproduction organs. Further research will be needed to fully uncover the Dsx mechanism in *Nasonia* that achieves the refined developmental regulation of male genitalia at specific time points, and to confirm whether NvDsx is required in females for female reproductive organ differentiation.

Visualizing *Dsx*-expressing cells in *D. melanogaster* has demonstrated that *Dsx* gene expression is under elaborate temporal and spatial control to regulate tissue-specific sexual differentation (Robinett et al., 2010). Here, we build on this knowledge by using a non-drosophilid species to show that different morphological characteristics require their own specific Dsx timing and action, and we suggest that this timing and action is species-specific. Our findings solidify the view that in insects, sexual development is not only a set and forget mechanism that only operates during embryogenesis, but one that requires continuous input from Dsx on a species-specific basis.

Data availability

The datasets generated during and/or analysed during the current study are available in the figshare repository, [10.6084/m9.figshare.15028191].

Author contributions

All authors contributed to conceptualization and methodology; Y.W., E.C.V., A.H.R, U.F, and M.C.R performed the investigation; Y.W. performed visualisation; Y.W. wrote the original draft; E.C.V, L.v.Z, reviewed and edited the draft; E.C.V., L.v.Z and C.T. supervised and managed the project and E.C.V. obtained funding.

Declaration of competing interest

The authors declare no competing interests.

Acknowledgment

We thank Dr. Hans Smid for assisting with phenotype recording; Rutger Diepeveen for his contribution to the *NvDsx* RNAi work; Joan Diaz Calafat, Age Muller, Simon Pleiter and Romy Gielings for their contribution to the *NvtraF* RNAi work; Min Xu for supporting the sample preparation, collection and measuring; and Weizhao Sun for recording the mating behavior of RNAi treated males. This work is part of the Dutch Research Council (NWO) research programme Innovational Research Incentives Scheme Veni with project number 863.13.014 granted to ECV.

Appendix A. Supplementary data

Supplementary data to this article can be found online at https://doi.org/10.1016/j.ibmb.2022.103724.

References

Ahmad, S.M., Baker, B.S., 2002. Sex-specific deployment of FGF signaling in *Drosophila* recruits mesodermal cells into the male genital imaginal disc. Cell 109, 651–661. https://doi.org/10.1016/S0092-8674(02)00744-4.

An, W., Cho, S., Ishii, H., Wensink, P.C., 1996. Sex-specific and non-sex-specific oligomerization domains in both of the *doublesex* transcription factors from *Drosophila melanogaster*. Mol. Cell Biol. 16, 3106–3111. https://doi.org/10.1128/MCB.16.6.3106.

Baker, B.S., Wolfner, M.F., 1988. A molecular analysis of *doublesex*, a bifunctional gene that controls both male and female sexual differentiation in *Drosophila melanogaster*. Genes Dev. 2, 477–489. https://doi.org/10.1101/gad.2.4.477.

Barmina, O., Kopp, A., 2007. Sex-specific expression of a HOX gene associated with rapid morphological evolution. Dev. Biol. 311, 277–286. https://doi.org/10.1016/J.YDBIO.2007.07.030.

Bopp, D., Saccone, G., Beye, M., 2014. Sex determination in insects: variations on a common theme. Sex. Dev. 8, 20–28. https://doi.org/10.1159/000356458.

Burtis, K.C., Baker, B.S., 1989. *Drosophila doublesex* gene controls somatic sexual differentiation by producing alternatively spliced mRNAs encoding related sex-specific polypeptides. Cell 56, 997–1010. https://doi.org/10.1016/0092-8674(89)90633-8.

Burtis, K.C., Coschigano, K.T., Baker, B.S., Wensink, P.C., 1991. The Doublesex proteins of *Drosophila melanogaster* bind directly to a sex-specific yolk protein gene enhancer. EMBO J. 10, 2577–2582. https://doi.org/10.1002/j.1460-2075.1991.tb07798.x.

Camara, N., Whitworth, C., Dove, A., van Doren, M., 2019. Doublesex controls specification and maintenance of the gonad stem cell niches in *Drosophila*. Development 146, dev170001. https://doi.org/10.1242/dev.170001.

Chaverra-Rodriguez, D., Dalla Benetta, E., Heu, C.C., Rasgon, J.L., Ferree, P.M., Akbari, O.S., 2020. Germline mutagenesis of *Nasonia vitripennis* through ovarian delivery of CRISPR-Cas9 ribonucleoprotein. Insect Mol. Biol. 29, 569–577. https://doi.org/10.1111/imb.12663.

Chen, S.-L., Dai, S.-M., Lu, K.-H., Chang, C., 2008. Female-specific *doublesex* dsRNA interrupts yolk protein gene expression and reproductive ability in oriental fruit fly, *Bactrocera dorsalis* (Hendel). Insect Biochem. Mol. Biol. 38, 155–165. https://doi.org/10.1016/j.ibmb.2007.10.003.

Chen, X., Cao, Y., Zhan, S., Tan, A., Palli, S.R., Huang, Y., 2019. Disruption of sex-specific *doublesex* exons results in male- and female-specific defects in the black cutworm, *Agrotis ipsilon*. Pest Manag. Sci. 75, 1697–1706. https://doi.org/10.1002/ps.5290.

Cho, S., Huang, Z.Y., Zhang, J., 2007. Sex-specific splicing of the honeybee *doublesex* gene reveals 300 million years of evolution at the bottom of the insect sex-determination pathway. Genetics 177, 1733–1741. https://doi.org/10.1534/genetics.107.078980.

Christiansen, A.E., Keisman, E.L., Ahmad, S.M., Baker, B.S., 2002. Sex comes in from the cold: the integration of sex and pattern. Trends Genet. 18, 510–516. https://doi.org/10.1016/S0168-9525(02)02769-5.

Clough, E., Jimenez, E., Kim, Y.A., Whitworth, C., Neville, M.C., Hempel, L.U., Pavlou, H. J., Chen, Z.X., Sturgill, D., Dale, R.K., Smith, H.E., Przytycka, T.M., Goodwin, S.F., VanDoren, M., Oliver, B., 2014. Sex- and tissue-specific functions of *Drosophila doublesex* transcription factor target genes. Dev. Cell 31, 761–773. https://doi.org/10.1016/j.devcel.2014.11.021.

Darling, D.C., Werren, J.H., 1990. Biosystematics of *Nasonia* (Hymenoptera: pteromalidae): two new species reared from birds' nests in North America. Ann. Entomol. Soc. Am. 83, 352–370. https://doi.org/10.1093/aesa/83.3.352.

DeFalco, T.J., Verney, G., Jenkins, A.B., McCaffery, J.M., Russell, S., Van Doren, M., 2003. Sex-specific apoptosis regulates sexual dimorphism in the *Drosophila* embryonic gonad. Dev. Cell 5, 205–216. https://doi.org/10.1016/S1534-5807(03)00204-1.

Garcia-Bellido, A., Merriam, J.R., 1971. Parameters of the wing imaginal disc development of *Drosophila melanogaster*. Dev. Biol. 24, 61–87. https://doi.org/10.1016/0012-1606(71)90047-9.

Geuverink, E., Beukeboom, L.W., 2014. Phylogenetic distribution and evolutionary dynamics of the sex determination genes *doublesex* and *transformer* in insects. Sex. Dev. 8, 38–49. https://doi.org/10.1159/000357056.

Godfray, H.C.J., 1994. Parasitoids: Behavioral and Evolutionary Ecology, Parasitoids: Behavioral and Evolutionary Ecology. Princeton University Press.

Gotoh, H., Miyakawa, H., Ishikawa, A., Ishikawa, Y., Sugime, Y., Emlen, D.J., Lavine, L. C., Miura, T., 2014. Developmental link between sex and nutrition; *doublesex* regulates sex-specific mandible growth via juvenile hormone signaling in stag beetles. PLoS Genet. 10, e1004098 https://doi.org/10.1371/journal.pgen.1004098.

Hamilton, W.D., 1967. Extraordinary sex ratios. Science 156, 477–488. https://doi.org/10.1126/science.156.3774.477, 80-.

Hoshijima, K., Inoue, K., Higuchi, I., Sakamoto, H., Shimura, Y., 1991. Control of *doublesex* alternative splicing by *transformer* and *transformer-2* in *Drosophila*. Science 252, 833–836. https://doi.org/10.1126/science.1902987, 80-.

Ito, Y., Harigai, A., Nakata, M., Hosoya, T., Araya, K., Oba, Y., Ito, A., Ohde, T., Yaginuma, T., Niimi, T., 2013. The role of *doublesex* in the evolution of exaggerated horns in the Japanese rhinoceros beetle. EMBO Rep. 14, 561–567. https://doi.org/10.1038/embor.2013.50.

Keisman, E.L., Baker, B.S., 2001. The *Drosophila* sex determination hierarchy modulates *wingless* and *decapentaplegic* signaling to deploy dachshund sex-specifically in the genital imaginal disc. Development 128, 1643–1656.

Keisman, E.L., Christiansen, A.E., Baker, B.S., 2001. The sex determination gene *doublesex* regulates the A/P organizer to direct sex-specific patterns of growth in the *Drosophila* genital imaginai disc. Dev. Cell 1, 215–225. https://doi.org/10.1016/S1534-5807(01)00027-2.

Kerkis, J., 1931. The growth of the gonads in *Drosophila melanogaster*. Genetics 16, 212–224.

Kijimoto, T., Moczek, A.P., Andrews, J., 2012. Diversification of *doublesex* function underlies morph-, sex-, and species-specific development of beetle horns. Proc. Natl. Acad. Sci. U. S. A 109, 20526–20531. https://doi.org/10.1073/pnas.1118589109.

Klein, A., Schultner, E., Lowak, H., Schrader, L., Heinze, J., Holman, L., Oettler, J., 2016. Evolution of social insect polyphenism facilitated by the sex differentiation cascade. PLoS Genet. 12, e1005952 https://doi.org/10.1371/journal.pgen.1005952.

Kopp, A., 2011. *Drosophila* sex combs as a model of evolutionary innovations. Evol. Dev. 13, 504–522. https://doi.org/10.1111/j.1525-142X.2011.00507.x.

Kopp, A., Duncan, I., Carroll, S.B., 2000. Genetic control and evolution of sexually dimorphic characters in *Drosophila*. Nature 408, 553–559. https://doi.org/10.1038/35046017.

Kunte, K., Zhang, W., Tenger-Trolander, A., Palmer, D.H., Martin, A., Reed, R.D., Mullen, S.P., Kronforst, M.R., 2014. *Doublesex* is a mimicry supergene. Nature 507, 229–232. https://doi.org/10.1038/nature13112.

Li, M., Au, L.Y.C., Douglah, D., Chong, A., White, B.J., Ferree, P.M., Akbari, O.S., 2017. Generation of heritable germline mutations in the jewel wasp *Nasonia vitripennis* using CRISPR/Cas9. Sci. Rep. 7, 1–7. https://doi.org/10.1038/s41598-017-00990-3.

Liu, N.-Y., Wu, G.-X., Ze, S.-Z., Yang, B., Zhu, J.-Y., 2017. Morphology and ultrastructure of the male reproductive system of the jewel wasp, *Nasonia vitripennis* (Walker) (Hymenoptera: pteromalidae). J. Asia Pac. Entomol. 20, 577–582. https://doi.org/10.1016/j.aspen.2017.03.017.

Loehlin, D.W., Enders, L.S., Werren, J.H., 2010a. Evolution of sex-specific wing shape at the widerwing locus in four species of *Nasonia*. Heredity 104, 260–269. https://doi.org/10.1038/hdy.2009.146.

Loehlin, D.W., Oliveira, D.C.S.G., Edwards, R., Giebel, J.D., Clark, M.E., Cattani, M.V., van de Zande, L., Verhulst, E.C., Beukeboom, L.W., Muñoz-Torres, M., Werren, J.H., 2010b. Non-coding changes cause sex-specific wing size differences between closely related species of *Nasonia*. PLoS Genet. 6, e1000821 https://doi.org/10.1371/journal.pgen.1000821.

Loehlin, D.W., Werren, J.H., 2012. Evolution of shape by multiple regulatory changes to a growth gene. Science 335, 943–947. https://doi.org/10.1126/science.1215193.

Lynch, J.A., 2015. The expanding genetic toolbox of the wasp *Nasonia vitripennis* and its relatives. Genetics 199, 897–904. https://doi.org/10.1534/GENETICS.112.147512.

Lynch, J.A., Desplan, C., 2006. A method for parental RNA interference in the wasp *Nasonia vitripennis*. Nat. Protoc. 1, 486–494. https://doi.org/10.1038/nprot.2006.70.

Massey, J.H., Wittkopp, P.J., 2016. The genetic basis of pigmentation differences within and between *Drosophila species*. Curr. Top. Dev. Biol. 119, 27–61. https://doi.org/10.1016/bs.ctdb.2016.03.004.

Mine, S., Sumitani, M., Aoki, F., Hatakeyama, M., Suzuki, M.G., 2021. Effects of functional depletion of *Doublesex* on male development in the sawfly, *Athalia rosae*. Insects 12, 849. https://doi.org/10.3390/INSECTS12100849.

Mine, S., Sumitani, M., Aoki, F., Hatakeyama, M., Suzuki, M.G., 2017. Identification and functional characterization of the sex-determining gene *doublesex* in the sawfly, *Athalia rosae* (Hymenoptera: tenthredinidae). Appl. Entomol. Zool. 52, 497–509. https://doi.org/10.1007/s13355-017-0502-3.

Miyakawa, M.O., Tsuchida, K., Miyakawa, H., 2018. The *doublesex* gene integrates multi-locus complementary sex determination signals in the Japanese ant, *Vollenhovia emeryi*. Insect Biochem. Mol. Biol. 94, 42–49. https://doi.org/10.1016/J.IBMB.2018.01.006.

Morrow, J.L., Riegler, M., Frommer, M., Shearman, D.C.A., 2014. Expression patterns of sex-determination genes in single male and female embryos of two *Bactrocera* fruit fly species during early development. Insect Mol. Biol. 23, 754–767. https://doi.org/10.1111/imb.12123.

Mysore, K., Sun, L., Tomchaney, M., Sullivan, G., Adams, H., Piscoya, A.S., Severson, D. W., Syed, Z., Duman-Scheel, M., 2015. siRNA-mediated silencing of *doublesex* during female development of the dengue vector mosquito *Aedes aegypti*. PLoS Neglected Trop. Dis. 9, e0004213 https://doi.org/10.1371/journal.pntd.0004213.

Nipitwattanaphon, M., Wang, J., Ross, K.G., Riba-Grognuz, O., Wurm, Y., Khurewathanakul, C., Keller, L., 2014. Effects of ploidy and sex-locus genotype on gene expression patterns in the fire ant *Solenopsis invicta*. Proc. R. Soc. B Biol. Sci. 281, 20141776. https://doi.org/10.1098/rspb.2014.1776.

Ohbayashi, F., Suzuki, M.G., Mita, K., Okano, K., Shimada, T., 2001. A homologue of the *Drosophila doublesex* gene is transcribed into sex-specific mRNA isoforms in the silkworm, *Bombyx mori*. Comp. Biochem. Physiol. B Biochem. Mol. Biol. 128, 145–158. https://doi.org/10.1016/S1096-4959(00)00304-3.

Oliveira, D.C.S.G., Werren, J.H., Verhulst, E.C., Giebel, J.D., Kamping, A., Beukeboom, L. W., van de Zande, L., 2009. Identification and characterization of the *doublesex* gene of *Nasonia*. Insect Mol. Biol. 18, 315–324. https://doi.org/10.1111/j.1365-2583.2009.00874.x.

Price, D.C., Egizi, A., Fonseca, D.M., 2015. The ubiquity and ancestry of insect *doublesex*. Sci. Rep. 5, 1–9. https://doi.org/10.1038/srep13068.

Ramakers, C., Ruijter, J.M., Deprez, R.H.L., Moorman, A.F., 2003. Assumption-free analysis of quantitative real-time polymerase chain reaction (PCR) data. Neurosci. Lett. 339, 62–66. https://doi.org/10.1016/S0304-3940(02)01423-4.

Raychoudhury, R., Desjardins, C.A., Buellesbach, J., Loehlin, D.W., Grillenberger, B.K., Beukeboom, L., Schmitt, T., Werren, J.H., 2010. Behavioral and genetic characteristics of a new species of <i>Nasonia<i/&gt. Heredity 104, 278–288. https://doi.org/10.1038/hdy.2009.147.

Robinett, C.C., Vaughan, A.G., Knapp, J.-M., Baker, B.S., 2010. Sex and the single cell. II. There is a time and place for sex. PLoS Biol. 8, e1000365 https://doi.org/10.1371/journal.pbio.1000365.

Shukla, J.N., Nagaraju, J., 2010a. *Doublesex*: a conserved downstream gene controlled by diverse upstream regulators. J. Genet. https://doi.org/10.1007/s12041-010-0046-6.

Shukla, J.N., Nagaraju, J., 2010b. Two female-specific DSX proteins are encoded by the sex-specific transcripts of *dsx*, and are required for female sexual differentiation in two wild silkmoth species, *Antheraea assama* and *Antheraea mylitta* (Lepidoptera, Saturniidae). Insect Biochem. Mol. Biol. 40, 672–682. https://doi.org/10.1016/J.IBMB.2010.06.008.

Shukla, J.N., Palli, S.R., 2012. Doublesex target genes in the red flour beetle. *Tribolium castaneum*. Sci. Rep. 2, 948. https://doi.org/10.1038/srep00948.

Slifer, E.H., 1969. Sense organs on the antenna of a parasitic wasp, *Nasonia vitripennis* (Hymenoptera, pteromalidae). Biol. Bull. 136, 253–263. https://doi.org/10.2307/1539818.

Snodgrass, R.E., 1957. A revised interpretation of the external reproductive organs of male insects. Smithsonian Misc. Collect. 135, 1–60.

Suzuki, M.G., Funaguma, S., Kanda, T., Tamura, T., Shimada, T., 2005. Role of the male BmDSX protein in the sexual differentiation of *Bombyx mori*. Evol. Dev. 7, 58–68. https://doi.org/10.1111/j.1525-142X.2005.05007.x.

Tamura, K., Dudley, J., Nei, M., Kumar, S., 2007. MEGA4: molecular evolutionary genetics analysis (MEGA) software version 4.0. Mol. Biol. Evol. 24, 1596–1599. https://doi.org/10.1093/molbev/msm092.

True, J.R., 2003. Insect melanism: the molecules matter. Trends Ecol. Evol. 18, 640–647. https://doi.org/10.1016/J.TREE.2003.09.006.

Ugajin, A., Matsuo, K., Kubo, R., Sasaki, T., Ono, M., 2016. Expression profile of the sex determination gene *doublesex* in a gynandromorph of bumblebee. *Bombus ignitus*. Sci. Nat. 103, 17. https://doi.org/10.1007/s00114-016-1342-7.

Verhulst, E.C., Beukeboom, L.W., van de Zande, L., 2010a. Maternal control of haplodiploid sex determination in the wasp *Nasonia*. Science 328, 620–623. https://doi.org/10.1126/science.1185805, 84).

Verhulst, E.C., van de Zande, L., 2015. Double nexus-*Doublesex* is the connecting element in sex determination. Brief. Funct. Genom. 14, 396–406. https://doi.org/10.1093/bfgp/elv005.

Verhulst, E.C., van de Zande, L., Beukeboom, L.W., 2010b. Insect sex determination: it all evolves around *transformer*. Curr. Opin. Genet. Dev. 20, 376–383. https://doi.org/10.1016/j.gde.2010.05.001.

Werren, J.H., Loehlin, D.W., Giebel, J.D., 2009. Larval RNAi in *Nasonia* (parasitoid wasp). Cold Spring Harb. https://doi.org/10.1101/pdb.prot5311. Protoc. 2009, pdb.prot5311.

Werren, J.H., Richards, S., Desjardins, C.A., Niehuis, O., Gadau, J., Colbourne, J.K., Nasonia Genome Working Group, A., 2010. Functional and evolutionary insights from the genomes of three parastoid *Nasonia* species. Science 327, 343–348. https://doi.org/10.1126/science.1178028, 84.

Whitworth, C., Jimenez, E., van Doren, M., 2012. Development of sexual dimorphism in the *Drosophila* testis. Spermatogenesis 2, 129–136. https://doi.org/10.4161/spmg.21780.

Williams, T.M., Selegue, J.E., Werner, T., Gompel, N., Kopp, A., Carroll, S.B., 2008. The regulation and evolution of a genetic switch controlling sexually dimorphic traits in *Drosophila*. Cell 134, 610–623. https://doi.org/10.1016/J.CELL.2008.06.052.

Xu, J., Zhan, S., Chen, S., Zeng, B., Li, Z., James, A.A., Tan, A., Huang, Y., 2017. Sexually dimorphic traits in the silkworm, *Bombyx mori*, are regulated by *doublesex*. Insect Biochem. Mol. Biol. 80, 42–51. https://doi.org/10.1016/J.IBMB.2016.11.005.

Zhuo, J.-C., Hu, Q.-L., Zhang, H.-H., Zhang, M.-Q., Jo, S.B., Zhang, C.-X., 2018. Identification and functional analysis of the *doublesex* gene in the sexual development of a hemimetabolous insect, the brown planthopper. Insect Biochem. Mol. Biol. 102, 31–42. https://doi.org/10.1016/j.ibmb.2018.09.007.